Waste Management 33 (2013) 347–355

Contents lists available at SciVerse ScienceDirect

Waste Management

journal homepage: www.elsevier.com/locate/wasman

Monte-Carlo human health risk assessment of mercury emissions from a MSW gasification plant

Giovanni Lonati [a,*], Francesca Zanoni [b]

[a] Dipartimento di Ingegneria Idraulica, Ambientale, Infrastrutture viarie, Rilevamento, Politecnico di Milano, P.zza L. da Vinci, 32 – 20133 Milano, Italy
[b] Airprotech srl, Viale Lombardia, 33 – 20013 Magenta, Italy

ARTICLE INFO

Article history:
Received 9 March 2012
Accepted 18 October 2012
Available online 22 November 2012

Keywords:
MSW gasification
Risk assessment
Mercury
Speciated mercury emissions
Probabilistic approach
Monte Carlo simulation

ABSTRACT

The potential impact of the atmospheric emission of mercury from a new waste gasification plant is assessed by means of a probabilistic approach based on probability density functions for the description of the input data (namely, emission rate of mercury gaseous and particulate species) and the model parameters involved in the individual risk exposure assessment through the pathways of inhalation, soil ingestion, dermal contact, and diet. The use of probability functions allowed the uncertainty in the input data and model parameters to be accounted for; the uncertainty was propagated throughout the evaluation by Monte Carlo technique, resulting in the probability distributions for the ambient air and soil concentrations nearby the plant and for the subsequent individual risk, estimated in terms of hazard index for both an adult and a child receptor. The estimated median concentration levels in air and soil are respectively in the 1.6×10^{-3}–2.2×10^{-2} ng m^{-3} range and in the 3.5×10^{-4}–1.7×10^{-2} mg kg^{-1} range, that is at least two orders of magnitude lower than the current background concentration in the ambient air and one order of magnitude lower than the concentration locally measured in the soil. The diet pathway is responsible for the most part (>80%) of the daily mercury intake, which, however, is at least four (median estimated values) and three orders (estimates for a reasonable maximum exposure) lower than the reference dose in the most part of the modeling domain. According to the locally measured background mercury levels in air and soil the additional contribution of the plant emissions to the environmental mercury levels appears of small significance, with an almost negligible impact on the hazard index for the population living in the neighborhood of the plant.

1. Introduction

Mercury is a highly mobile environmental pollutant toxic to both humans and wildlife at extremely low concentration levels (WHO, 1991). In recent years, a growing attention concerned atmospheric mercury and a number of projects have been carried out in the United States and in Europe with the main goal to improve the knowledge on sources, fluxes, behavior and impacts of mercury in the environment (Pacyna et al., 2006b; U.S. EPA, 1997a). In particular, the attention was focused on the assessment of anthropogenic mercury emissions to the atmosphere, with specific address for combustion facilities including municipal solid waste (MSW) thermochemical conversion processes like incineration, pyrolysis and gasification (Pacyna et al., 2006b; Carpi, 1997; Kilgroe, 1996; Hall et al., 1991). In particular, MSW gasification has been looked at the MSW advanced thermal treatment of the near future (Malkow, 2004; Defra, 2007) also in Europe, where incineration is still the most commonly applied thermal process. Differently from Japan, where gasification is largely utilized, in Europe only a few plants, and some of these as demonstrator plants, have been operating with MSW; furthermore, some of these plants encountered problems in complying with emission limits (e.g.: Isle of Wight Demonstrator plant, UK) or in the regular continuous operation (Fondotoce di Verbania Demonstrator plant, Italy), that led to the plant retrofitting into conventional incineration process or to the plant dismantlement. Nevertheless, gasification plants are still proposed for selected MSW thermal processing as for the project presented in this case study.

Mercury stack emissions from thermal conversion of waste are thought to include both vapor and particulate forms: vapor-phase mercury emissions include both the elemental (Hg^0) and the oxidized chemical form $(Hg^{2+})_V$, while particle-phase mercury emissions are composed primarily of oxidized compounds $(Hg^{2+})_P$ due to the relatively high vapor pressure of elemental mercury (U.S. EPA, 1997a). Organic mercury in the form of methyl mercury was generally not found in stack gases from combustion sources (Pacyna et al., 2006a; Munthe et al., 2003). At the combustion chamber temperature (>800 °C) most compounds of mercury decompose to vapor-phase elemental mercury in the exhaust gas

* Corresponding author. Tel.: +39 02 23996430; fax: +39 02 23996499.
E-mail address: giovanni.lonati@polimi.it (G. Lonati).

0956-053X/$ - see front matter © 2012 Elsevier Ltd. All rights reserved.
http://dx.doi.org/10.1016/j.wasman.2012.10.015

stream (Lindqvist, 1986; Schroeder and Jackson, 1985; Otani et al., 1984); as the flue gas cools, elemental mercury reacts with other flue gas constituent and is oxidized to reactive species like HgO, $HgCl_2$ and $HgSO_4$ (Carpi, 1997) eventually condensing on the surface of the ash particles (Hirt et al., 1990). The mercury oxidized forms produced by these reactions, reactive gaseous mercury $Hg(^{2+})_V$ and particulate reactive mercury $Hg(^{2+})_P$, are collectively referred as reactive mercury. The temperature of the flue gas and the type of emission control equipments, together with other factors like the concentration of particulate carbon and other pollutants in the exhaust stream or the concentration of mercury in the feed material, can further influence the speciation of mercury in the combustion gas (Carpi, 1997; Hall et al., 1990).

The impact of the mercury atmospheric emissions is usually evaluated by means of environmental impact assessment (EIA) studies developed in order to quantify the associated risk for the human health. In particular, European Union regulations require the EIA for the projects of new plants for the thermal treatment of waste (EU Directive 85/337/EEC, 1985). These studies are usually performed following an approach based on deterministic values for input data, namely for the pollutant emission rate, and for the risk model parameters. However this approach often leads to the evaluation of conservative conditions, where the stack emissions are usually equal to the maximum regulatory value, thus producing overestimated risk values actually associated with low probability of occurrence. Furthermore, the exposure models within the risk assessment model (Zemba et al., 1996; Belcher and Travis, 1991; Levin, 1991; McKone and Bogen, 1991) require a relative broad set of input parameters affected by both epistemic and stochastic uncertainty (or natural variability). The former, named "uncertainty", consists in a lack of knowledge regarding the true value of a parameter while the latter, named "variability", derives from the intrinsic variation of the data value (Ripamonti et al., 2011; Kumar et al., 2009).

This study is intended to assess the impacts of mercury emissions from a new municipal solid waste gasification plant, recently proposed for the realization South-East of the city of Milan in Italy, by developing the impact assessment procedure in probabilistic terms. The impacts are evaluated first in terms of the concentration of mercury in the ambient air and in the soil in the neighbourhood of the plant and then in terms of the additional risk for the human health deriving from the intake of mercury through the exposure pathways of direct inhalation of contaminated air, soil ingestion, soil dermal contact, and diet. The probabilistic approach allows dealing with the uncertainty issue of the evaluation by representing both epistemic and stochastic uncertainty of all the model components (i.e.: the stack emissions and the model parameters of the exposure pathways) through probability density functions (PDFs) and propagating the uncertainty through the impact assessment model by Monte-Carlo technique. While the probabilistic risk assessment for the emission of carcinogenic pollutants from waste thermal treatment plants has been proposed in literature (Schuhmacher et al., 2001; Sonnemann et al., 2002; Meneses et al., 2004; Lonati et al., 2007a; Kumar et al., 2009), to our knowledge this is one of the few works where the probabilistic approach has been applied throughout the whole mercury risk assessment model (Constantinou et al., 1995). The evaluation specifically considers the emission, atmospheric transport, and ground deposition to the soil of the main mercury forms, allowing to assess the spatial distribution of their concentrations in the air and soil and the subsequent risk for the human health in terms of PDFs. The estimated ambient air and soil concentrations are compared to the existing mercury levels that can be considered representative for the study area based on monitoring campaigns measurements performed in Milan area.

Together with maps for the air and soil concentration patterns, GIS mapping of the estimated risk is produced for a more powerful communication of the study results. For the area most affected by the emissions of the plant the risk distributions estimated by the probabilistic approach are compared with the risk values derived from the conventional deterministic assessment and the propagation of the uncertainty of the input data and of the model parameters is evaluated by the decomposition of the risk variance.

2. Materials and methods

The risk assessment model consists of three main sub-models applied in cascade: an emission assessment model, an atmospheric dispersion model, and an exposure and individual risk model. Input data and model parameters have been defined as probability distribution functions (PDFs) to account for their uncertainty. The software package Crystal Ball (Version 4.0) was used to propagate the uncertainty throughout the whole risk assessment model, resulting in final PDFs for the estimated mercury concentrations and related individual risk. Crystal Ball uses a Monte-Carlo simulation in order to propagate the distributions calculating the risk several thousand times by randomly drawing values from the probability distribution functions of the input data and the model parameters (Decisioneering, 1996).

2.1. Gasification plant features

The plant in project is designed for a daily waste throughput of 900 metric tons, split in three separate lines. Waste is fed to the plant as RDF (refuse derived fuel) produced from the mechanical biological treatment of both raw municipal solid waste (150 Mg d^{-1}) and of the unsorted residual dry fraction left downstream of urban waste separate collection (750 Mg d^{-1}); the gasification reactor is designed based on a RDF lower heating value of 16 MJ kg^{-1}.

Despite the waste pre-treatment, the RDF fed to the plant can still contain mercury, mainly as a consequence of improper disposal of button cell batteries and bulb lamps. In fact, even though the average mercury concentration of the feed stream to thermal plants decreased considerably during the last decades thanks to a considerable reduction of the application of mercury and to the introduction of effective battery return systems, presently the mercury concentration in municipal solid waste is still in the orders of 1–2 mg kg^{-1} approximately (van Veizen et al., 2002). However, during thermal processing mercury passes practically for 100% in the flue gas, thus leading to serious environmental concerns both at the local (Muenhor et al., 2009) and global scale (Seigneur et al., 2004).

The plant in project operates according to the heat gasifier configuration based on the "High Temperature Gasifying and Direct Melting Reactor" process technology, proposed by JFE Engineering Company (Japan). The gasification process is carried out in a moving bed downdraft shaft-furnace coupled with a process integrated melting of the slag: as the feed descends through the furnace, it is gasified and its inorganic components are melted to slag, tapped at the bottom of the shaft while the gas product is combusted in an adjoining boiler to generate steam used to generate electricity in a steam turbine (Themelis, 2008; Arena, 2012; Tanigaki et al., 2012)

The flue gas treatment line is configured with a centrifugal separator followed by a first fabric filtration unit for dust removal, a dry sorption reactor for acidic gases and organic trace pollutants removal through sodium bicarbonate and activate carbon injection, a second fabric filtration unit for sorption by-products removal, and final Selective Catalytic Removal DeNOx; flue gas is then released into the atmosphere through a 42-m tall stack.

2.2. Emission estimation model

The aim of the emission estimation model is to assess the mass flow rate of speciated mercury emitted by the waste gasification plant. The mass flow rate Q ($g\,s^{-1}$) of total mercury released in the atmosphere is estimated based on the plant daily throughput P ($Mg_{waste}\,day^{-1}$), on the flue gas specific production V_F ($m^3 \cdot Mg_{waste}^{-1}$), and on the total mercury concentration at the stack C_{Hg} ($mg\,m^{-3}$):

$$Q = \frac{C_{Hg} \cdot P \cdot V_F}{24 \cdot 3600} \quad (1)$$

While P takes a deterministic value corresponding to the plant design data ($900\,Mg_{waste}\,d^{-1}$), C and V_F are affected by uncertainty due to the inherent variability in the combustion process and in the composition of the gasified waste. PDFs derived from literature data have been used to describe these variables because the gasification plant of this study is not yet in operation. Since literature data for the specific gas production are scarce, V_F is described by a triangular PDF distribution, ranging between the minimum ($3360\,m^3\,Mg_{waste}^{-1}$) and the maximum ($6670\,m^3\,Mg_{waste}^{-1}$) of the literature data (Barducci et al., 1997; Choy et al., 2004) and with mode equal to the plant design value ($5420\,m^3\,Mg_{waste}^{-1}$).

Literature data for the total mercury stack concentration are more frequent (CE-CERT, 2009; Giuliano et al., 2008; Khoo, 2008; Adlhoch and Sato, 2000; Calaminus and Stahlberg, 1998; Larson et al., 1996), allowing statistical analyses for their description by fitting a theoretical distribution model. After the detection and elimination of outliers through Grubbs' test (Grubbs, 1969), the best fitting PDF for C_{Hg} was individuated in an exponential distribution (parameter rate = 47.85), according to the Kolmogorov–Smirnov test at $\alpha = 0.1$ significance level. For the subsequent calculations, however, this distribution was truncated at the concentration value ($0.05\,mg\,m^{-3}$) set by the current European regulation for waste incinerators (EU Directive 2000/76/EC).

The total mercury emission Q was subsequently split between the particle ($Hg(^{2+})_P$) and the vapor phase, this latter in turn split between elemental mercury ($Hg(^0)$) and divalent mercury ($Hg(^{2+})_V$), through partitioning coefficients derived from literature data for the emission of waste thermal treatment plants (U.S. EPA, 2005, 1997a; Yuan et al., 2005; Cohen et al., 2004; Munthe et al., 2003; Carpi, 1997; Pacyna and Munch, 1991; Hall et al., 1990). According to these data the most part of mercury (about 60% on the average) is emitted as vapor-phase $Hg(^{2+})_V$ whereas $Hg(^0)$ and $Hg(^{2+})_P$ respectively account for about 27% and 13% of the total emission. The PDFs describing the partitioning coefficients (Supplementary material, Table S1) have been combined with the PDF for the total mercury emission Q estimated by Eq. (1) leading to the PDFs for the emission mass flow rates of the three forms of mercury described by the theoretical models summarized in Table 1.

2.3. Atmospheric dispersion, ground deposition and soil concentration model

The aim of this sub-model is to estimate the ambient air concentration at ground level, the ground deposition, and the subsequent concentration in the soil due to the atmospheric deposition processes for each single grid cell of the calculation domain, a squared area (10×10 km) centered on the plant and regularly subdivided in 1600 cells (40×40 cells, 250 m cell size). The calculation domain is a flat area mainly characterized by rural land use (80%); however some urbanized areas are also present in correspondence with the small towns located in the Northern part of the domain.

The atmospheric dispersion was simulated through the Lagrangian puff dispersion model CALPUFF (Scire et al., 2000), a multi-layer non steady state puff dispersion model designed to model the dispersion of gases and particles using space and time varying meteorology based on similarity equations, turbulence, emission strengths, atmospheric transformation and removal. CALPUFF model was applied using meteorological data, required in term of time sequence of three-dimensional fields of velocity, wind direction and temperature, and two-dimensional fields of micrometeorological parameters describing the stability of atmosphere, prepared by CALMET processor from data measured by the regional meteorological monitoring network. Thanks to its ability to simulate situations of calm wind periods, CALPUFF is very suitable to model the atmospheric dispersion in the area, most part of the year characterized by poor ventilation.

Based on the speciated mass flow rates PDFs reported in Table 1, CALPUFF simulations produced as outputs the PDFs of the annual average concentration C_a ($ng\,m^{-3}$) for both the total and the speciated mercury in the ambient air; these speciated outputs allowed a more accurate assessment of the mercury ground deposition, taking into account the different deposition behaviors of the mercury forms.

The annual ground deposition flux D_{tot}, resulting from the contribution of both the dry (D_{dry}) and the wet (D_{wet}) deposition flux, has been calculated for each of the mercury forms by the following general equation:

$$D_{tot} = D_{dry} + D_{wet} = C_a \cdot v_d + C_a \cdot W \cdot H \cdot FU \quad (2)$$

Dry deposition is calculated based on the dry deposition velocity v_d (particle or vapor phase) and on the corresponding ground level concentration C_a produced by CALPUFF; wet deposition based on the washout coefficient W, on the annual mean rainfall depth H, on the fraction of rainy year FU, and on the ground level concentration C_a. The PDFs used for the parameters in Eq. (2) are summarized in Table 2; these distributions have been directly derived from the statistical analysis of literature data, namely for the dry deposition velocity for mercury vapor phase and for the washout coefficients, and of local meteorological data, for the annual rainfall depth and for the fraction of rainy year.

For elemental mercury ($Hg(^0)$) only the dry deposition was accounted for: in fact, because of its low solubility in water $Hg(^0)$ is not efficiently incorporated into the wet deposition (washout coefficient range 10–100) and its contribution to the total deposition flux can be neglected (Selin et al., 2007; Cohen et al., 2004). Conversely, oxidized mercury forms $Hg(^{2+})_V$ and $Hg(^{2+})_P$ may be deposited rather quickly and close to the emission source through both dry and wet deposition processes (Schroeder and Munthe, 1998). For the dry deposition velocity of vapor-phase $Hg(^{2+})_V$ no measurements or predictions have been reported in literature; however, according to several authors (Marsik et al., 2007;

Table 1
Probability density functions of the mercury mass flow rates ($g\,s^{-1}$) emitted in vapor and particulate phase. (Gamma [L = Location, *Sc* = Scale, *Sh* = Shape]).

Mercury form	Distribution model and parameters	
	Vapor phase	Particulate phase
$Hg^{(0)}$	Gamma $L = 2.27 \times 10^{-8}$, $Sc = 4.27 \times 10^{-9}$, $Sh = 0.815$	–
$Hg^{(2+)}$	Gamma $L = 1.16 \times 10^{-7}$, $Sc = 1.84 \times 10^{-3}$ $Sh = 0.905$	Gamma $L = 1.40 \times 10^{-8}$, $Sc = 2.11 \times 10^{-4}$ $Sh = 0.806$

Table 2
Probability density functions for air and soil concentrations at the most exposure site. (*G* = Gamma [Scale, Shape], *LN* = Lognormal [geometric mean, geometric standard deviation]).

Mercury form	Air concentration C_a ($ng\,m^{-3}$)	Soil concentration C_s ($mg\,kg^{-1}$)
Total mercury Hg	*G* [3.33×10^{-2}, 0.959]	*LN* [1.75×10^{-2}, 4.94]
Elemental mercury $Hg(^0)$	*G* [1.22×10^{-2}, 0.819]	*G* [2.90×10^{-4}, 0.587]
Oxidized mercury $Hg(^{2+})_V$	*G* [5.31×10^{-2}, 0.893]	*G* [5.66×10^{-2}, 0.595]
Oxidized mercury $Hg(^{2+})_P$	*G* [6.00×10^{-3}, 0.811]	*G* [1.22×10^{-2}, 0.628]

Bullock and Brehme, 2002; U.S. EPA, 1997a; Constantinou et al., 1995), the dry deposition velocity of gaseous nitric acid can be used $Hg(^{2+})_V$ because of their similar behavior: in fact, $Hg(^{2+})_V$ and HNO_3 have a solubility on the same order of magnitude and comparable affinity for organic matter in soils (Grigal, 2003; Kordel et al., 1997).

The PDF for the deposition velocity of the particulate mercury $Hg(^{2+})_P$ has been estimated based on the particle size distribution of the particulate matter emitted by the plant. This distribution was derived from literature data for waste thermal treatment plants equipped with fabric filtration units as for the gasification plant of this case study; in fact, lacking specific literature references for the waste gasification technology, the most influence on the particle size distribution can be assumed to be associated with the flue gas treatment line configuration for particulate matter. Size-resolved dry deposition velocities, estimated through specific equations for particle deposition (Sakata et al., 2006; Schwede and Paumier, 1997; Noll and Fang, 1989; Sehmel and Hodgson, 1978), has been combined based on the particle size distribution leading to an overall particle deposition velocity described by a Gamma distribution (Table S2), whose parameters take different values according to the features of the deposition surface (urban or rural land use).

Total mercury concentration in soil has been estimated accounting for both the vapor and particle phase deposition and for the loss from soil by several mechanisms, including leaching, erosion, runoff and volatilization; a first-order decay equation is usually adopted to describe the overall effect of these loss mechanisms that reduce the soil concentration determined by the deposition (U.S. EPA, 2005). The integration of the mass balance equation for mercury in the soil over the period of plant operation leads to the following formulation for the soil concentration C_s ($mg\,kg^{-1}$):

$$C_s = \frac{\sum_i D_{tot,i} \cdot [1 - \exp(-k_s \cdot T)]}{z \cdot k_s \cdot BD} \quad i = Hg(^0), Hg(^{2+})_V, Hg(^{2+})_P \qquad (3)$$

The PDF of the mercury concentration in soil C_s ($mg\,kg^{-1}$) was determined based on the PDFs reported in Table S3 for the soil bulk density BD ($g\,cm^{-3}$), the soil loss constant k_s ($years^{-1}$), the soil mixing depth z (cm), and for the period of plant operation T (years) derived from the statistical analysis of literature data.

2.4. Exposure and human health risk assessment model

The individual exposure and the subsequent health risk for the people living in the study area has been computed according to the conventional procedure (U.S. EPA, 2005), taking into account the different exposure pathways through which an individual can be potentially exposed: direct inhalation of air, dermal absorption, ingestion of contaminated soil, and ingestion of contaminated vegetables through the diet. Only the consumption of contaminated vegetables locally grown was considered within the diet pathway since no breeding or fishing activities are present in the area around the plant.

The following general equation for calculating the daily intake of mercury I ($mg_{Hg}\,kg_{bw}\,d^{-1}$) per unit mass of body weight:

$$I = \frac{C \cdot CR \cdot EF \cdot ED}{BW \cdot AT} \qquad (4)$$

has been applied in probabilistic terms, that is based on PDFs for all the parameters involved (Table S4). In Eq. (4) C is the total mercury concentration previously estimated, i.e. C_a ($ng\,m^{-3}$) for air and C_s ($mg\,kg^{-1}$) for soil, CR is the air/soil consumption rate, namely the amount of contaminated medium consumed per unit time ($m^3\,d^{-1}$ for air, $kg\,d^{-1}$ for soil), EF (dimensionless) and ED (years) are the exposure frequency and duration, BW (kg) the individual body weight, and AT (years) the averaging period of the exposure.

The consumption rate CR takes in turn the meaning of the inhalation rate IR (inhalation pathway), of the soil-skin contact rate (dermal absorption pathway), of the soil ingestion rate (ingestion pathway), and of the consumption rate of mercury contaminated vegetables (diet pathway). Actually, the soil-skin contact rate is evaluated through the exposed skin area surface S and the soil-skin adherence factor AD; furthermore, both the dermal absorption and the ingestion pathway consider the actual absorption through the absorption factors AF_{da} and AF_{ing}, respectively.

The contamination of the locally grown vegetables was assessed through the bioconcentration factors (BCFs) that reflect the extent of the mercury partitioning between plants and the environmental media (air and soil). However, since for the leafy, above-ground parts of the plants, virtually the entire mercury uptake is from air (Mosbæk et al., 1988), the soil-vegetable BCF takes values close to zero. In the study area there aren't specific vegetable cultivations, however domestic vegetable plots with different home-grown produce are present: therefore PDFs for the BCFs have been derived based on literature data for various plant species, leading to a rather wide range of BCFs values.

The daily intake of mercury was calculated separately for each single cell according to its land use (urban or rural) and considering both an adult and a child receptor, typically characterized by a greater exposure through the pathway of soil ingestion (U.S. EPA, 1997b). Based on the conservative assumption that the actual dose is equal to the estimated overall intake, the risk for the human health was subsequently quantified in terms of the hazard index HI (dimensionless), given by the ratio between the daily intake I and the reference dose RfD. In fact, since mercury is responsible for non-carcinogenic effects, the standard risk assessment models assume a level of exposure below which no adverse effects are expected, namely the RfD ($mg_{Hg}\,kg_{bw}\,d^{-1}$), that is the daily intake estimated to determine no appreciable risk of adverse health effects over lifetime. Due to the few literature data available for the reference dose, for this latter parameter a deterministic value of $3{\cdot}10^{-4}\,mg_{Hg}\,kg_{bw}\,d^{-1}$ was considered in this study accordingly with WHO recommendations (U.S. EPA, 2005; OEHHA, 2002).

3. Results and discussion

3.1. Spatial distribution of air and soil concentrations

For each single grid cell of the calculation domain, the outputs of the CALPUFF dispersion model are the PDFs of the annual average concentrations of total and speciated mercury in air. CALPUFF simulations have been performed for ten different years, leading to PDFs that account for both the variability of the emission rate and of the meteorological conditions in the area. These PDFs belong to the same theoretical model (i.e.: the 3-parameter Gamma model)

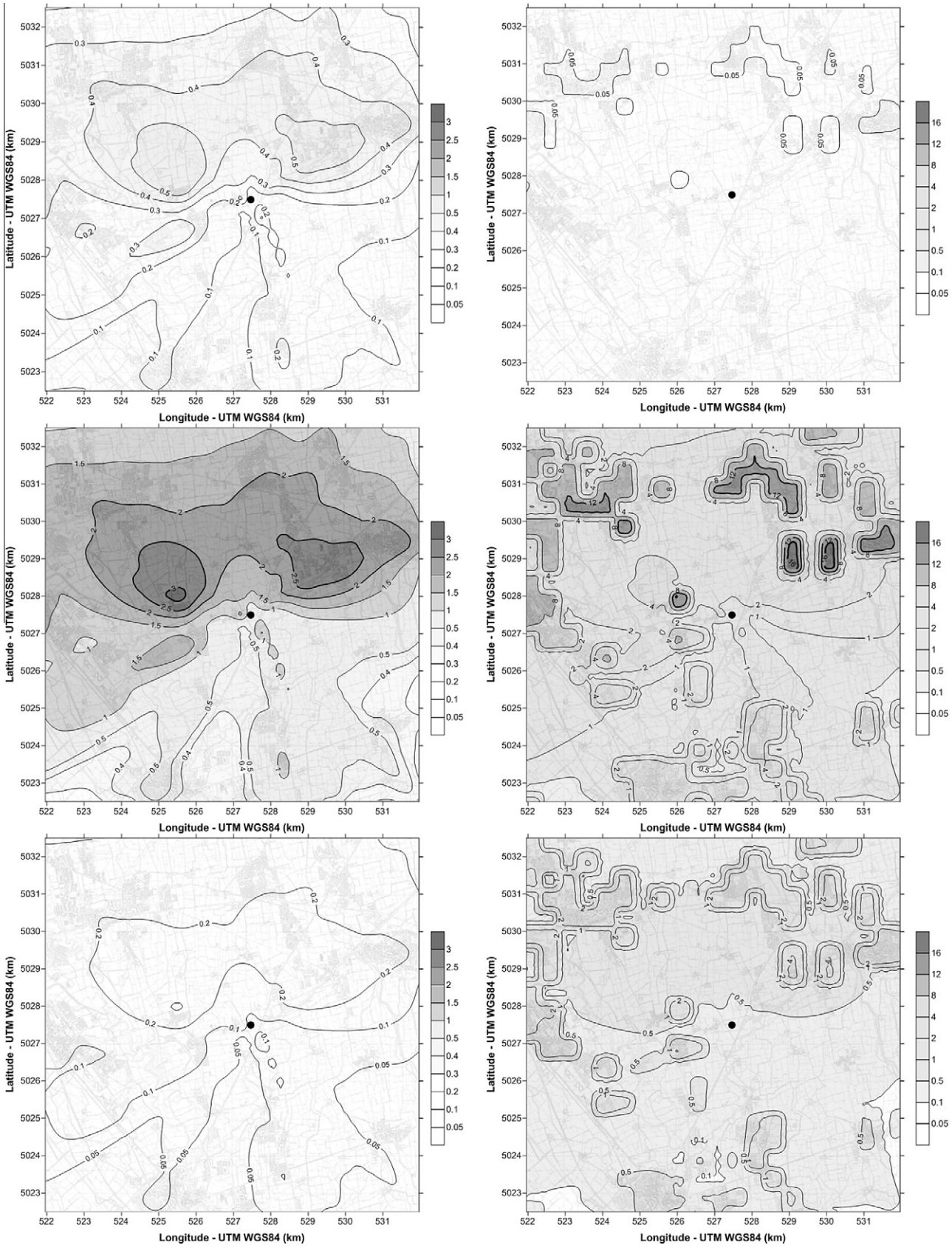

Fig. 1. Spatial distribution of the 50th percentile of the PDFs for air (left column: 10^{-2} ng m^{-3}) and soil concentration (right column: 10^{-3} mg kg^{-1}): $Hg(^0)$ in the upper panel, $Hg(^{2+})_V$ in the middle panel, and $Hg(^{2+})_P$ in the lower panel.

with cell-by-cell variable values for the location and scale parameter and a same value in the whole area for the shape parameter of the distribution. These results allow drawing maps of the estimated concentrations or, more specifically, to draw iso-concentration contour maps for given statistical parameters or percentiles of the concentration distributions. As an example, the maps in Fig. 1 display the spatial distribution of the 50th percentile of the ground level concentration in ambient air for each mercury form: $Hg(^0)$, $Hg(^{2+})_V$ and $Hg(^{2+})_P$ estimated values are in the 4.7×10^{-4}–6.3×10^{-3}, 2.3×10^{-3}–3.1×10^{-2}, and 2.2×10^{-4}–3.1×10^{-3} ng m^{-3} range, respectively. Coherently with the partitioning at the emission, $Hg(^{2+})_V$ levels are about 5 and 10 times higher than those of $Hg(^0)$ and $Hg(^{2+})_P$, with particulate phase mercury accounting for only 15% of the total mercury concentration. Consistently with the local wind rose (Fig. S1), the maps show that the areas most affected by the emissions of the plant are located North-East and North-West to the plant; in fact, Southern winds are usually associated with unstable atmospheric conditions leading to rather high concentrations close to the emission point whereas, conversely, the winds blowing from North-East occur under stable conditions, thus determining low ground-level concentrations in the study area.

The soil concentration modeling outputs consist of the PDFs for the soil concentration of speciated mercury. As for the air, the PDFs for the soil concentration belong to the 3-parameter gamma model, still with cell-by-cell variable values for the location and scale, but with the shape parameter taking different values for cells with rural (about 80% of the study area) and urban land use, in correspondence with the small towns located in the Northern part of the study area. The 50th percentile soil concentration maps reported in Fig. 1 clearly highlight the different behavior in the ground deposition of the mercury forms: in fact, despite its higher emission rate $Hg(^0)$ levels in the soil are almost two orders of magnitude lower than those of $Hg(^{2+})_P$. The 50th percentile of the concentrations estimated in the soil is in the 1.7×10^{-6}–8.8×10^{-5}, 3.5×10^{-4}–1.7×10^{-2}, and 6.8×10^{-5}–4.1×10^{-3} mg kg^{-1} range, for $Hg(^0)$, $Hg(^{2+})_V$ and $Hg(^{2+})_P$ respectively.

The highest concentrations for both the air and the soil are estimated for an urban grid cell at about 2 km from the plant in the North-Eastern direction: the parameters of the distributions obtained for this cell are summarized in Table 2 for the total and speciated mercury concentration in ambient air and soil.

The estimated mercury concentrations in the ambient air and soil can be interpreted in the light of the existing concentration levels in the study area. For the air concentration, lacking local data, the interpretation can rely on total vapor-phase mercury data from monitoring campaigns performed in the outskirts of Milan (Lonati et al., 2007b). Based on these data an annual average of 1 ng m^{-3} can be reasonably assumed for the study area. The additional contribution to mercury levels in the ambient air due to the plant emission is therefore rather small: in fact, the 50th percentile of the estimated concentrations (1.6×10^{-3}–2.2×10^{-2} ng m^{-3} range), is at least two orders of magnitude lower than the current background concentration, and also the upper percentiles (99th) of the estimated distributions, ranging between 1.1×10^{-2}–1.5×10^{-2} ng m^{-3}, are more than one order lower than the measured values. Regarding the soil concentration, local data ranging between 0.02 and 0.5 mg kg^{-1} suggest an average reference value of 0.21 mg kg^{-1} (Saponaro et al., 2005). As for the air concentration the impact of the plant emissions is rather insignificant: the estimated 50th percentile of the total mercury concentration in the soil (3.5×10^{-4}–1.7×10^{-2} mg kg^{-1} range) is at least one order of magnitude lower than the average and only the maximum values of the highest percentiles (>99th) take values comparable with the maximum measured data.

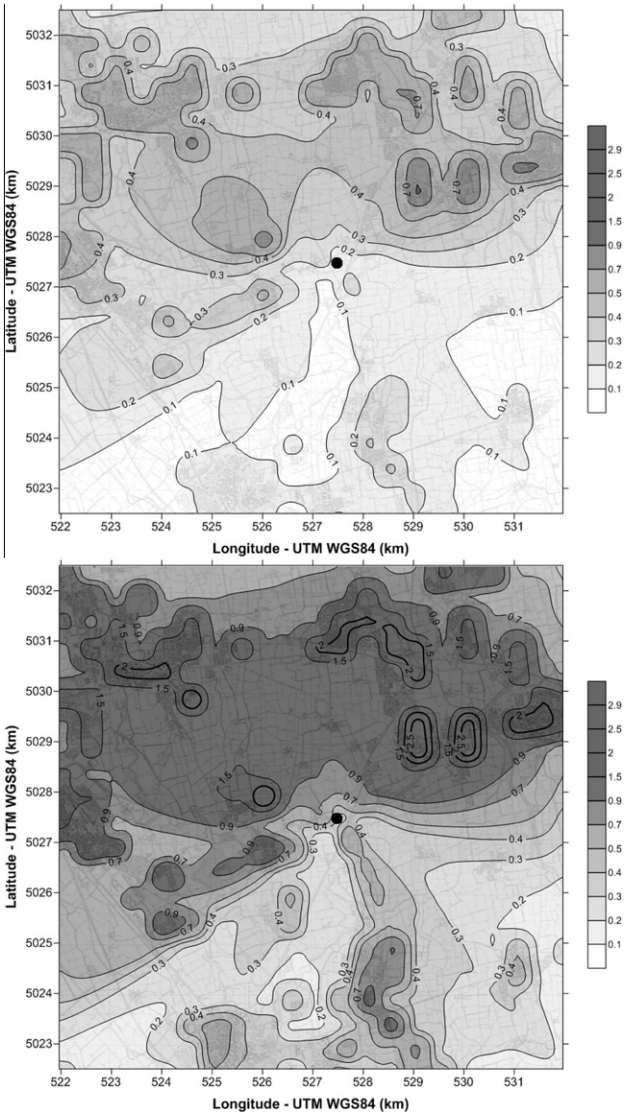

Fig. 2. Spatial distribution of the reasonable maximum values of the estimated individual risk (hazard index HI) for the adult (upper panel) and child receptor (lower panel). Risk values to be multiplied by 10^{-3}.

Table 3
Relative contributions to the maximum risk value of each exposure pathway (A = Adult, C = Child).

Pathway	Relative contributions to the total risk	
	Probabilistic approach (%)	Deterministic approach (%)
Inhalation	A: 22.5 C: 10.9	A: 4.4 C: 7.8
Dermal absorption	A: 7.3 C: 8.4	A: 2.7 C: 17.5
Soil ingestion	A: 6.1 C: 16.2	A: 0.4 C: 8.4
Diet	A: 64.0 C: 64.5	A: 92.4 C: 66.2

3.2. Spatial distribution of the individual risk

Probabilistic simulations through the risk assessment model produced PDFs for the incremental individual risk, expressed in

term of the hazard index (HI), for each cell of the calculation domain considering both an adult and a child receptor. The ranges of the median HI values in the study area are 6.53×10^{-6}–1.26×10^{-4} for the adult and 1.69×10^{-5}–3.77×10^{-4} for the child receptor; this means that the highest median daily intake of mercury is lower than the reference dose of about four orders of magnitude for both the receptors. Due to the higher intake of contaminated soil through the soil ingestion pathway, accordingly with the behavior of some young children, referred to as "pica" children (U.S. EPA, 1997b), to intentionally eat soil, higher HI values have been obtained for the child receptor.

As shown in the maps of Fig. 2, the HI values for the reasonable maximum exposure risk, individuated by the 90th percentile of the PDFs (Schuhmacher et al., 2001), are always at least three orders of magnitude lower than the reference dose for the adult (HI < 0.001); for the child receptor HI values are about 3 times higher but still less than 0.001 in the most part of the modeling domain.

The PDFs for the HI estimated at the grid cell where the maximum air and soil concentrations are expected belong to the 2-parameter lognormal model: geometric mean and standard deviation values are respectively 1.26×10^{-4} and 4.67 for the adult receptor and 3.77×10^{-4} and 4.83 for the child receptor.

The risk assessment was also performed by the conventional deterministic approach, based on single conservative point values for all the model components and, in particular, assuming a mercury stack concentration value (0.05 mg m^{-3}) equal to the current EU regulatory limits of for waste incinerator emissions. The maximum values of the deterministic HI estimates (3.38×10^{-3} and 4.04×10^{-3} for adult and child receptor, respectively) are more than one order of magnitude higher than the median values resulting from the probabilistic assessment and approximately corresponding to the 98th and 93th percentile of the hazard index PDFs.

The conservative assumptions adopted in the conventional deterministic approach for compensating, at least partially, the lack of knowledge about the parameters uncertainty and variability, led thus to rather high estimates of the risk.

3.3. Sensitivity analysis

Sensitivity analyses have been performed in order to assess the relative contribution to the risk of the exposure pathways and to investigate the contribution to the risk variance of each single input variable and model parameter involved in the risk assessment procedure.

Table 3 reports the relative contributions of the exposure pathways to the maximum individual risk estimated: the diet pathway is responsible for the most part (65%) of the risk for both the receptors, followed by inhalation (22%) for the adult and by soil

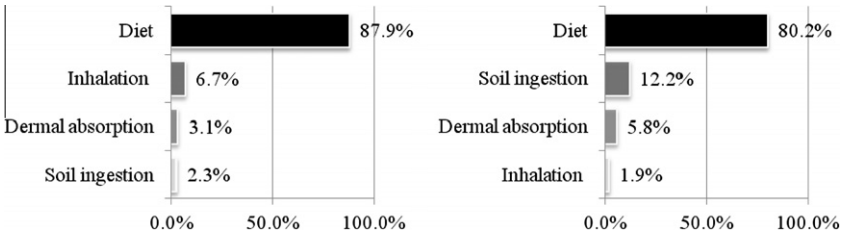

Fig. 3. Contribution to the risk variance of each exposure pathway for the adult (left) and the child (right) receptor.

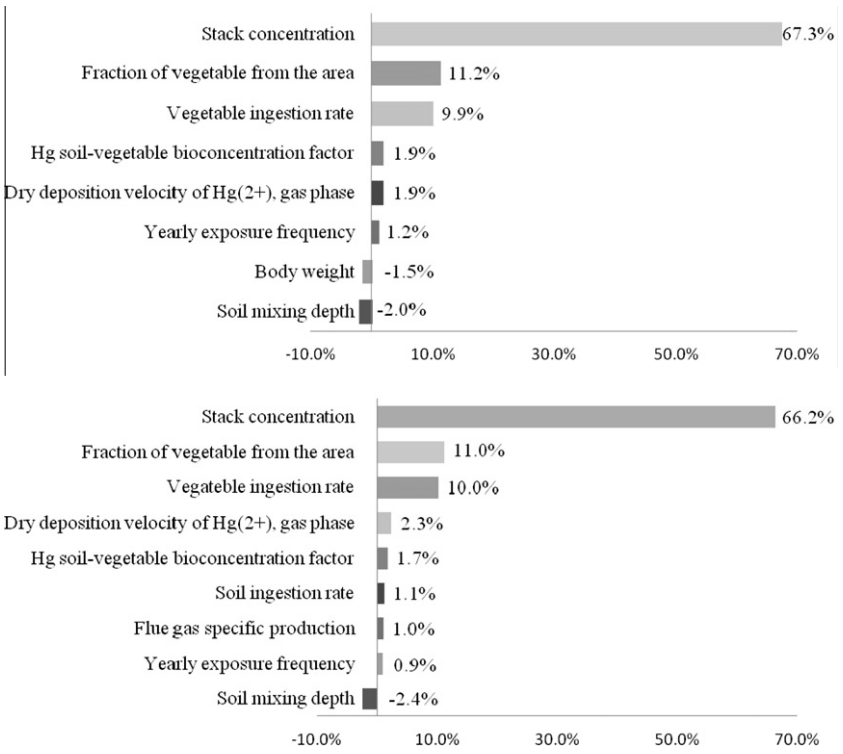

Fig. 4. Variance decomposition of the estimated risk for the adult (upper panel) and child receptor (lower panel).

ingestion (16%) for the child. The more relevant role of the soil ingestion and dermal adsorption pathways, still determined by the contact with contaminated soil, is consistent with the already mentioned higher soil intake of children.

The estimated predominant contribution of the diet is in agreement with literature data, where, however, its relative contribution is normally much higher (>80% for an adult receptor and >65% for a child, as reported by Cangialosi et al., 2008) due to the mercury intake through contaminated fish (Wolkin et al., 2012). Simply considering the ingestion of contaminated vegetables, diet is responsible for a reduced relative contribution to the final risk, but still largely prevailing on the other pathways.

It is worth noticing that the results of the deterministic approach provide rather different contributions to the total risk, especially for the adult receptor: while for the child the relative contributions are rather similar to those of the probabilistic approach, conversely for the adult receptor the diet contribution rises up from 64% to more than 90%, thus largely reducing the contributions of the other pathways. This result is essentially driven by the wide range of values for the air-vegetable BCF: the choice of a conservative value for this latter parameter results in the larger influence of the diet pathway.

The results of the sensitivity analyses on the risk estimates are shown in Figs. 3 and 4 as tornado plots illustrating the decomposition of the risk variance among the exposure pathways and between the input variables and model parameters, respectively. Coherently with its prevailing contribution to the total risk, the diet is also the most influential pathway on the risk variance for both the adult and child receptor (88% and 80%, respectively); the lower contribution for the child receptor is due to the larger contribution of soil ingestion (12% vs. 2.3% for the adult).

The decomposition of the risk variance between the input variables and the model parameters points out that to increase the accuracy of the risk estimates efforts should primarily focus, regardless for the age of the receptor, on the mercury stack concentration, that contributes to the risk variance for about 65%, and, then on the parameters related to the diet pathway, namely on the fraction of vegetables form the area and on the vegetable ingestion rate, whose contribution to risk variance is about 20% overall.

4. Conclusion

The impact on ambient concentrations and the subsequent risk for the human health due to the atmospheric emissions of mercury from a new waste gasification plant has been assessed by means of a fully probabilistic approach. The speciated mercury emission rates and all the model parameters have been described by probability density functions and propagated through the assessment model by means of Monte Carlo simulations, leading to air and soil concentrations and health risk estimates expressed in terms of probability distributions that incorporate both the epistemic uncertainty and the aleatory variability. The median air concentration levels estimated in the study area are in the 1.6×10^{-3}–2.2×10^{-2} ng m^{-3} range for the air concentration and in the 3.5×10^{-4}–1.7×10^{-2} mg kg^{-1} for the soil concentration, that is at least one order of magnitude lower than the levels locally measured in air and soil. For the air concentration the upper percentiles of the estimated distributions are still more than one order lower than the measured values whilst for the soil concentration they take values comparable with the maximum measured data.

The additional risk for the human health is almost negligible: in fact, the highest median daily intake of mercury and the intake at the reasonable maximum exposure level are more than three orders of magnitude lower than the reference dose, at least. The resulting hazard index values estimated at the most impacted point in the study area are described by a 2-parameter lognormal model with geometric mean and standard deviation values respectively equal to 1.26×10^{-4} and 4.67 for the adult, and 3.77×10^{-4} and 4.83 for the child receptor. According to these distributions, the conventional deterministic approach for risk assessment, typically based on conservative point values for all the model components and on the regulatory limits for mercury stack concentration, provides very conservative results, approximately corresponding to the 98th and 93th percentile of the hazard index PDFs and more than one order of magnitude higher than the median values resulting from the probabilistic assessment.

The probabilistic approach also allowed performing sensitivity analyses in order to decompose the estimated risk variance among the exposure pathways and between the input variables and model parameters involved in the risk assessment procedure. Coherently with its prevailing contribution to the total risk (65%), the diet is also the most influential pathway on the risk variance for both the adult and child receptor (88% and 80%, respectively). The parameters related to the diet pathway, namely the fraction of vegetables form the area and the vegetable ingestion rate, contribute to risk variance for about 20% overall; however, in order to increase the accuracy of the risk estimates, the efforts should primarily focus on the mercury stack concentration, which contributes to the risk variance for about 65% regardless for the age of the receptor.

Appendix A. Supplementary material

Supplementary data associated with this article can be found, in the online version, at http://dx.doi.org/10.1016/j.wasman.2012.10.015.

References

Adlhoch, W., Sato, H., 2000. High-temperature winkler gasification of municipal solid waste. In: Proceeding of 2000 Gasification Technologies Conference, San Francisco, California, October 8–11.

Arena, U., 2012. Process and technological aspects of municipal solid waste gasification. A review. Waste Manage. 32, 625–639.

Barducci, G.L., Ulivieri, P., Polzinetti, G.C., Donati, A., Repetto, F., 1997. New developments in biomass utilisation for electricity and low energy gas production, on the gasification plant of Greve in Chianti – Florence, development in exploitation of LEG from BF and RDF. In: Bridgwater, A.V., Boocock, D.G.B. (Eds.), Developments in Thermochemical Biomass Conversion, vol. 2. Blackie Academic & Professional, London, United Kingdom, pp. 1045–1057.

Belcher, G.D., Travis, C.C., 1991. Health Effects of Municipal Waste Incineration. CRC Press, 211–235.

Bullock, O.R., Brehme, K.A., 2002. Atmospheric mercury simulation using the CMAQ model: formulation description and analysis of wet deposition results. Atmos. Environ. 26, 2135–2146.

Calaminus, B., Stahlberg, R., 1998. Continuous in-line gasification/vitrification process for thermal waste treatment: process technology and current status of project. Waste Manage 18, 547–556.

Cangialosi, F., Intini, G., Liberti, L., Notarnicola, M., Stellacci, P., 2008. Health risk assessment of air emissions from a municipal solid waste incinerator plant – a case study. Waste Manage 28, 885–895.

Carpi, A., 1997. Mercury from combustion sources: a review of the chemical species emitted and their transport in the atmosphere. Water Air Soil Poll. 98, 241–254.

CE-CERT, 2009. Evaluation of Emissions from Thermal Conversion Technologies Processing Municipal Solid Waste and Biomass. Final report Prepared by University of California at Riverside's College of Engineering-Center for Environmental Research and Technology for BioEnergy Producers Association. (<http://socalconversion.org/pdfs/UCR> Emissions Report 62109).

Choy, K.K.H., Porter, J.F., Hui, C.-W., McKay, G., 2004. Process design and feasibility study for small scale MSW gasification. Chem. Eng. J. 105, 31–41.

Cohen, M., Artz, R., Draxler, R., Miller, P., Poissant, L., Niemi, D., Rattè, D., Deslauriers, M., Duval, R., Laurin, R., Slotnick, J., Nettesheim, T., McDonald, J., 2004. Modeling the atmospheric transport and deposition of mercury to the Great Lakes. Environ. Res. 95, 247–265.

Constantinou, E., Gerath, M., Mitchell, D., Seigneur, C., Levin, L., 1995. Mercury from power plants: a probabilistic approach to the evaluation of potential health risks. Water Air Soil Poll. 80, 1129–1138.

Decisioneering, 1996. Crystal BallTM Version 4.0. Decisioneering Inc., Denver, Colorado.

Defra, 2007. Advanced thermal treatment of municipal solid waste. Enviros Consulting Limited on behalf of Department for Environment, Food & Rural Affairs (Defra), <www.defra.gov.uk>.

European Union Council Directive 85/337/EEC of 27 June 1985 on the assessment of the effects of certain public and private projects on the environment. Official Journal L 175, (05.07.85).
European Union, Directive 2000/76/EC of the European Parliament and of the council of 4 December 2000 on the incineration of waste. Official Journal of the European, Communities, L332/91.
Giuliano, M., Grosso, M., Rigamonti, L., 2008. Energy recovery from municipal waste: a case study for a middle-sized Italian district. Waste Manage 28, 39–50.
Grigal, D.F., 2003. Mercury sequestration in forests and peatlands: a review. J. Environ. Qual. 32, 393–405.
Grubbs, F.E., 1969. Procedures for detecting outlying observations in samples. Technometrics 11, 1–21.
Hall, B., Lindqvist, O., Ljungstrom, E., 1990. Mercury chemistry in simulated flue gases related to waste incineration conditions. Environ. Sci. Technol. 24, 108–111.
Hall, B., Schager, P., Lindqvist, O., 1991. Chemical reactions of mercury in combustion flue gases. Water Air Soil Poll. 56, 3–14.
Hirt, H., Lochum, J., Jodeit, H., 1990. A thermal process for decontaminating fly ash from waste incinerators. Chem. Eng. Technol. 12, 1054–1055.
Khoo, H.H., 2008. Life cycle impact assessment of various waste conversion technologies. Waste Manage 29, 1892–1900.
Kilgroe, J.D., 1996. Control of dioxin, furan, and mercury emissions from municipal soild waste combustors. J. Hazard Mater. 47, 163–194.
Kordel, W., Dassenakis, M., Lintelmann, J., Padberg, S., 1997. The importance of natural organic material for environmental processes in waters and soils. Pure Appl. Chem. 69, 1571–1600.
Kumar, V., Mari, M., Schumacher, M., Domingo, J.L., 2009. Partitioning total variance in risk assessment: application to a municipal solid waste incinerator. Environ. Modell. Softw. 24, 247–261.
Larson, E., Worrel, E., Chen, J., 1996. Clean fuels from municipal solid waste for fuel cell buses in metropolitan areas. Resour. Conserv. Recy. 17, 273–298.
Levin, A., 1991. Comparative analysis of health risk assessment for municipal waste combustors. J. Air Waste Manage. 41, 20–31.
Lindqvist, O., 1986. Fluxes of mercury in the Swedish environment: contributions from waste incineration. Waste Manage. Res. 4, 35–44.
Lonati, G., Cernuschi, S., Giugliano, M., Grosso, M., 2007a. Health risk analysis of PCDD/F emissions from MSW incineration: comparison of probabilistic and deterministic approaches. Chemosphere 67, 334–343.
Lonati, G., Ozgen, S., Giugliano, M., Cernuschi, S., 2007b. Atmospheric mercury in Milan area (Italy). In: Proc. 14th International Union of Air Pollution Prevention and Environmental Protection Associations (IUAPPA) World Congress 2007, Brisbane, Australia, 9–13, September.
Malkow, T., 2004. Novel and innovative pyrolysis and gasification technologies for energy efficient and environmentally sound MSW disposal. Waste Manage. 24, 53–79.
Marsik, F.J., Keeler, G.J., Landis, M.S., 2007. The dry deposition of speciated mercury to the Florida Everglades: measurements and modeling. Atmos. Environ. 41, 136–149.
McKone, T., Bogen, K., 1991. Predicting uncertainties in risk assessment. Environ. Sci. Technol. 25, 1674–1681.
Meneses, M., Schuhmacher, M., Domingo, J.L., 2004. Health risk assessment of emissions of dioxins and furans from a municipal waste incinerator: comparison with other emission sources. Environ. Int. 30, 481–489.
Mosbæk, H., Tjell, J.C., Sevel, T., 1988. Plant uptake of airborne mercury in background areas. Chemosphere 17, 1227–1236.
Muenhor, D., Satayavivad, J., Limpaseni, W., Parkpian, P., Delaune, R.D., Gambrell, R.P., Jugsujinda, A., 2009. Mercury contamination and potential impacts from municipal waste incinerator on Samui Island, Thailand. J. Environ. Sci. Health A 44, 376–387.
Munthe, J., Wangberg, I., Iverfeldt, A., Lindqvist, O., Stromberg, D., Sommar, J., Gardfeldt, K., Petersen, G., Ebinghaus, R., Prestbo, E., Larjava, K., Siemens, V., 2003. Distribution of atmospheric mercury species in Northern Europe: final results from the MOE project. Atmos. Environ. 37, S9–S20.
Noll, K.E., Fang, K.Y.P., 1989. Development of a dry deposition model for atmospheric coarse particles. Atmos. Environ. 23, 585–594.
OEHHA, 2002. Air Toxics Hot Spots Program Risk Assessment Guidelines: Part III, Technical Support Document for the Determination of Non-cancer Chronic Reference Exposure Levels. California Environmental Protection Agency, Office of Environmental Health Hazard.
Otani, Y., Emi, H., Kanaoka, C., Matsuit, S., 1984. Behavior of metal mercury in gases. Environ. Sci. Technol. 18, 793–796.
Pacyna, J.M., Munch, J., 1991. Anthropogenic mercury emission in Europe. Water Air Soil Poll. 56, 51–61.
Pacyna, E.G., Pacyna, J.M., Steenhuisen, F., Wilson, S., 2006a. Global anthropogenic mercury emission inventory for 2000. Atmos. Environ. 40, 4048–4063.
Pacyna, E.G., Pacyna, J.M., Fudala, J., Strzelecka-Jastrzab, E., Hlawiczka, S., Panasiuk, D., 2006b. Mercury emissions to the atmosphere from anthropogenic sources in Europe in 2000 and their scenarios until 2020. Sci. Total Environ. 370, 147–156.
Ripamonti, G., Lonati, G., Baraldi, P., Cadini, F., Zio, E., 2011. Uncertainty propagation methods in PCDD/F emission estimation models. In: Proceedings of the European Safety and Reliability Association, ESREL 2011 Annual Conference, Troyes, France, September 18–22.
Sakata, M., Marumoto, K., Marukawa, M., Asakura, K., 2006. Regional variations in wet and dry deposition fluxes of trace elements in Japan. Atmos. Environ. 46, 521–531.
Saponaro, S., Sezenna, E., Bonomo, L., 2005. Remediation actions by a risk assessment approach: a case study of mercury contamination. Water Air Soil Poll. 168, 187–212.
Schroeder, W.H., Jackson, R.A., 1985. An instrumental analytical technique for speciation of atmospheric mercury. Int. J. Environ. Anal. Chem. 22, 1–18.
Schroeder, W.H., Munthe, J., 1998. Atmospheric mercury – an overview. Atmos. Environ. 32, 809–822.
Schuhmacher, M., Meneses, M., Xifrò, A., Domingo, J.L., 2001. The use of Monte Carlo simulation techniques for risk assessment: study of a municipal waste incinerator. Chemosphere 43, 787–799.
Schwede, B.D., Paumier, O.J., 1997. Sensitivity of the industrial source complex model to input deposition parameters. J. Appl. Meteorol. 36, 1088–1095.
Scire, J.S., Strimaitis, D.G., Yamartino, R.J., 2000. A user guide for CALPUFF dispersion model. Earth Tech Inc., Concord, MA.
Sehmel, G.A., Hodgson, W.H., 1978. A Model for Predicting Dry Deposition of Particles and Gases to Environmental Surfaces, Battelle Pacific Northwest Laboratories, Richland, WA, PNL-SA-6721.
Seigneur, C., Vijayaraghavan, K., Lohman, K., Karamchandani, P., Scott‡, C., 2004. Global source attribution for mercury deposition in the United States. Environ. Sci. Technol. 38, 555–569.
Selin, N.E., Jacob, D.J., Park, R.J., Yantosca, R.M., Strode, S., Jaeglè, L., Jaffe, D., 2007. Chemical cycling and deposition of atmospheric mercury: global constraints from observations. J. Geophys. Res. 112, D02308.
Sonnemann, G.W., Pla, A., Schuhmacher, M., Castells, C., 2002. Framework for the uncertainty assessment in the impact pathway analysis with an application on a local scale in Spain. Environ. Int. 28, 9–18.
Tanigaki, N., Manako, K., Osada, M., 2012. Co-gasification of municipal solid waste and material recovery in a large-scale gasification and melting system. Waste Manage. 32, 667–675.
Themelis, N.J., 2008. Developments in thermal treatment technologies. In: Proceedings of NAWTEC16, 16th Annual North American Waste-to-Energy Conference, May 19–21, 2008, Philadelphia, Pennsylvania, USA.
U.S. EPA, 1997a. Mercury Study Report to Congress, Volume III: Fate and Transport of Mercury in the Environment. U.S. Environmental Protection Agency, Washington, DC, EPA/452/R-97/005.
U.S. EPA, 1997b. Exposure Factors Handbook (Final Report). U.S. Environmental Protection Agency, Washington, DC, EPA/600/P-95/002F a–c.
U.S. EPA, 2005. Human health risk assessment for hazardous waste combustion facilities. U.S. Environmental Protection Agency, Office of Solid Wastes, Washington, DC, Report EPA-530-R- 05–006.
van Veizen, D., Langenkamp, H., Herb, G., 2002. Review: mercury in waste incineration. Waste Manage. Res. 20, 556–568.
WHO, 1991. Environmental Health criteria 118: Inorganic mercury. World Health Organization, Geneva.
Wolkin, A., Hunt, D., Martin, C., Caldwell, K.L., McGeehin, M.A., 2012. Blood mercury levels among fish consumers residing in areas with high environmental burden. Chemosphere 86, 967–971.
Yuan, C.-S., Lin, H.-Y., Wu, C.-H., Liu, M.-H., 2005. Partition and size distribution of heavy metals in the flue gas from municipal soild waste incinerators in Taiwan. Chemosphere 59, 135–145.
Zemba, G.S., Green, C.L., Crouch, A.C., Lester, R.R., 1996. Quantitative risk assessment of stack emissions from municipal waste combustors. J. Hazard Mater. 47, 229–275.